Journal of Scientific Research & Reports
6(6): 476-482, 2015; Article no.JSRR.2015.172
ISSN: 2320-0227

SCIENCEDOMAIN *international*
www.sciencedomain.org

Microstructure and Composition Design of Magnetic Ni-Mn-Sn Co-sputter Deposited Films

A. Quintana-Nedelcos[1*], J. L. Sanchez-Llamazares[1], T. García-Fernández[2], S. Guvenc[3], M. Yumak[3] and C. García[3,4]

[1]*Department of Advanced Materials, San Luis Potosi Institute of Scientific Research and Technology, San Luis Potosí, México.*
[2]*Department of Physics, Autonomous University of Mexico City, México DF, México.*
[3]*Department of Physics, Bogaziçi University, Istanbul, Turkey.*
[4]*Department of Physics, Federico Santa María Technical University, Valparaiso, Chile.*

Authors' contributions

This work was carried out in collaboration between all authors. All authors read and approved the final manuscript.

Article Information

DOI: 10.9734/JSRR/2015/16672
Editor(s):
(1) Francisco Torrens, Institut Universitari de Ciència Molecular, Universitat de València, Edifici d'Instituts de Paterna, València, Spain.
Reviewers:
(1) Anonymous, Turkey.
(2) Anonymous, Japan.
(3) Anonymous, Turkey.
Complete Peer review History: http://www.sciencedomain.org/review-history.php?iid=967&id=22&aid=8613

Short Research Article

Received 10th February 2015
Accepted 10th March 2015
Published 28th March 2015

ABSTRACT

In this work, we study the effect of the substrate temperature (ST) during sputter-deposition as well as co-sputtering deposition on the fabrication of nanostructured Ni-Mn-Sn thin films. Sputtered films show Mn losses of around 10 at.% while the average grain size (<d>) increased from 30 nm to 105 nm with the increasing of ST. Mn losses compensation is proposed by co-sputtered deposition. With such a purpose a variable electrical power was applied to the radio frequency (RF) Mn cathode. By increasing the electrical power applied to the RF Mn cathode both Mn and Ni contents approach to the targeted nominal composition Ni:Mn:Sn = 50:37:13. Elemental chemical composition analyses show that the composition varied between $Ni_{61.5}Mn_{26.2}Sn_{12.3}$ and $Ni_{54.6}Mn_{30.5}Sn_{14.9}$ when the applied RF-power increased from 0 W to 30 W.

**Corresponding author: Email: arisqn@gmail.com;*

Keywords: Ni-Mn-Sn; magnetic shape memory alloys; sputtering; co-sputtering deposition.

1. INTRODUCTION

For well-selected compositional ranges, Heusler alloys, in the Ni-Mn-X (X= Ga, Sn, In, Sb) ternary systems, may exhibit two different magnetization jumps in which the magnetocaloric effect MCE can be achieved. These magnetization jumps are associated to: (i) the second-order ferromagnetic phase transition of the austenite phase and, (ii) the first-order martensitic transformation (MT) for which a large peak values of the magnetic entropy change has been reported [1,2]. This transition occurs in a narrow temperature range, and shows thermal hysteresis and large magnetic hysteresis losses on heating due to the field-induced reverse MT [3].

Looking for the development of cooling devices for nano and microsystems [4], thin films are particularly appropriate since the heat transfer may be strongly favored by their higher surface/volume ratio. Hence, cooling devices with high-frequency cooling cycles may be developing [5]. Many methods have been used for producing thin films; studies prove that the film growth technique has an important impact in the production of alloys thin films [6]. In such a sense, many efforts have been taken to study the technical parameters influence on the physical properties of the Ni-Mn-X (X: Ga, Sn, In, Sb) films alloys [7-17]. These studies have shown that the manipulation of individual technical parameters during the film deposition, usually affect to more than one physical property of the deposited films. For instance, it has been demonstrated that variations in the thickness and chemical composition of Ni-Mn-Ga films can be affected by the chamber pressure [11], target-substrate distance and deposition time [18]. The surface morphologies of twined areas in NiMnGa thin films is strongly affected by the composition of the film [15], and the MT shows a non-monotonic dependence with the film thickness [12]. In Ref. 8 was reported an increment of the austenitic grain size related to the increase of the substrate temperature without significant element losses in Ni-Mn-Sn based alloys. However, for thickness above 1400 nm the formation of $MnSn_2$ and Ni_3Sn_4 precipitates affects the structural order of the film [19]. Also, it has been established that in Ni-Mn-Sn ultrathin films the Curie temperature (Tc) of the austenitic (AST) phase is virtually independent of film thickness (t) and the Tc of the martensitic (MST) phase increase when t decrease [7]. For magnetron-sputtered Ni-Co-Mn-In thin films it was found that both target aging and increased substrate temperature result in elemental losses [14].

Summarizing, the deposition of high quality ferromagnetic shape memory alloys (FSMAs) films, i.e. with a desired microstructure and magnetic response for a given chemical composition is a difficult and challenging technical question. Regarding the chemical control, it has been proved that the co-sputtering deposition is a powerful technique for a precise tuning and control of the resulting film composition [20]. In this contribution we explore the possibility to deposit NiMnSn thin films with a desired composition, namely $Ni_{50}Mn_{37}Sn_{13}$, and a controlled microstructure. With such a purpose it has been separately studied the effect of the substrate temperature (ST) and co-sputtering deposition of NiMnSn sputtered films.

2. EXPERIMENTAL DETAILS

Two series of NiMnSn films, hereafter referred to as *series T* and *series CoS*, were deposited by means of the magnetron sputtering and co-sputtering technique on (100) silicon substrates. During deposition of both film series the high-vacuum sputtering chamber was initially evacuated to a base final pressure of $5x10^{-6}$Torr. Films were deposited in a highly pure Ar atmosphere at $3x10^{-2}$ Torr of chamber pressure and the substrate holder was rotated at 20 rpm.

Two targets, both supplied by Kurt J. Lesker Company, one of nominal composition of $Ni_{50}Mn_{37}Sn_{13}$ and the other one of pure Mn (99.95 %), were used and inserted in the DC and RF cathodes, respectively. For the T series the target was sputteredat 100 W for 45 min. The substrate temperature (ST) was varied from 200ºC up to 500ºC (i.e. ST = 200ºC, 300ºC, 400ºC, and 500ºC). The films of this series have been labeled as: T_200; T_300; T_400 and T_500 respectively. A co-sputtering process (series referred to as CoS) was proposed for compensating Mn evaporation losses. Films of CoS series were deposited applying a constant power of 100 W to the DC cathode and different powers to the RF cathode of pure Mn target, namely 0 W, 10 W, 20 W, and 30 W. The deposition time and ST were fixed at 45 min and 400ºC, respectively. The films of this series will be identified hereafter to as CoS_0, CoS_10, CoS_20, and CoS_30, respectively.

Microstructural characterization was done in a FIB DUAL BEAM FEI HELIOS 600 NANOLAB platform. SEM images of the typical microstructure of films were taken from both surface and cross section. More than 300 measurements were made to estimate average grain size <*d*> and film thickness. The latter was determined from the cross sectional SEM micrographs. Average chemical composition of deposited films was estimated by X-ray energy dispersive spectroscopy (EDS). To determine the elemental chemical composition, the EDS detector was calibrated with a bulk Ni-Mn-Sn sample of a known composition that was similar to that of the samples studied (i.e. $Ni_{50}Mn_{37}Sn_{13}$). Magnetization measurements were performed from 10 K to 350 K using a Quantum Design PPMS-9T Evercool-II® platform with the vibrating sample magnetometer module. Zero field cooling (ZFC), field cooling (FC), and field heating (FH) thermomagnetic curves were measured under an applied static magnetic field of μ_oH= 5 mT with a heating or cooling rate of 1 K/min.

3. RESULTS AND DISCUSSION

For films of *series T* the average atomic concentration for each element, together with the corresponding error bar is shown in Fig. 1(a). These results were based on more than 30 measurements for each film sample taken on the film surface. The standard deviation obtained for the elemental chemical composition (as determined by EDS) was 0.4 - 0.6 at.% for Ni, 0.4 - 0.6 at.% for Mn, and 0.3 - 0.4 at.% for Sn. The large difference found in the elemental chemical composition between the target and sputter films (~ 10 at.%) is mainly attributed to Mn deficiencies, and, is independent on the substrate temperature. The occurrence of Mn losses is consistent with previously published results for Ni-Co-Mn-In sputtered films [14]. In spite of the significant compositional shift, it must be emphasized that the element distribution in the films produced is quite homogenous. This result suggests that even when the attained composition noteworthy deviates from that of the sputtered target, the substrate temperature does not affect the resulting chemical composition of the resulting as-deposited films. In such a sense, an important parameter that strongly affects the MT temperature in Ni-Mn-Sn Heusler alloys is the average electron concentration per atom (*e/a*) [21,22], which is usually estimated from the resulting average chemical composition. Considering the number of valence electrons per atom for Ni, Mn, and Sn (i.e. 10, 7, and, 4, respectively), the calculated *e/a* for the films, referred to as T_200, T_300, T_400 and T_500, is 8.45, 8.45, 8.49, and 8.48, respectively. Hence, this parameter does not exhibit a significant variation.

Fig. 2 shows the typical SEM micrographs of the surface and fractured cross sectional of the *series T*. Images show that films exhibit a columnar-like microstructure. Measured average grain size <*d*> and its standard deviation are listed in Table 1. As expected, the increase of ST leads to the increase of <*d*>. The average film thickness <*t*>, estimated from the fractured cross-sectional SEM micrographs, was around 200 nm; notice, that ST does not significantly affect this parameter. This is a positive aspect concerning the deposition of Heusler films with a controlled nanostructure. However, the non-reproducibility of the target stoichiometry is a major problem that should be elucidated in order to produce films with a desired chemical composition. In this respect, the compensation of Mn loss by means of co-sputtering seems to be the most reliable practical solution [20].

Table 1. Average grain size <*d*> and the standard deviation for samples of *series T*

ST (^{o}C)	200	300	400	500
<*d*>(nm)	30	56	102	105
Std. Dev	7	17	30	27

The average atomic concentration for each element together with the corresponding error bar for the co-sputtered films (i.e. *series CoS*) is shown in Fig. 1(b). Notice that with the increasing of the electrical power applied to RF Mn cathode both the Mn and Ni content approach to the desired $Ni_{50}Mn_{37}Sn_{13}$ composition.

Typical SEM micrographs of the surface and fractured cross-sectional granular structure for films of the *series CoS* are shown in Fig. 3. As for the *series T*, all the films show a similar thickness of ~ 200 nm. Moreover, their average grain size (80 nm) and the grain columnar morphology seems to be independent of the power applied to the pure Mn target. Hence, this does not affect the microstrutural films characteristics. These results suggest that by means of a co-puttering deposition process one can synthesize Heusler thin films with a desired stoichiometry preserving their average grain size and thickness.

A preliminary magnetic characterization for the films of *series CoS* was carried out by measuring the temperature dependence of magnetization *M(T)*. Fig. 4 shows the *M(T)* curves measured in ZFC, FC and FH regimes from 10 K to 350 K under an applied magnetic field of 50 mT for the samples CoS_0 Fig. 4(a) and CoS_30 Fig. 4(b). The corresponding *dM/dT* vs. *T* curves are shown as inserted graphs. None of the curves reveal the occurrence of first-order martensite to austenite structural transition. The magnetic transition temperature, or Curie temperature T_C, of samples was inferred from the minimum of the *dM/dT* vs *T* curve. They were 290 K and 305 K for samples CoS_0 and CoS_30, respectively. The observed temperature shift should result from the *Tc* dependence with the film stoichiometry.

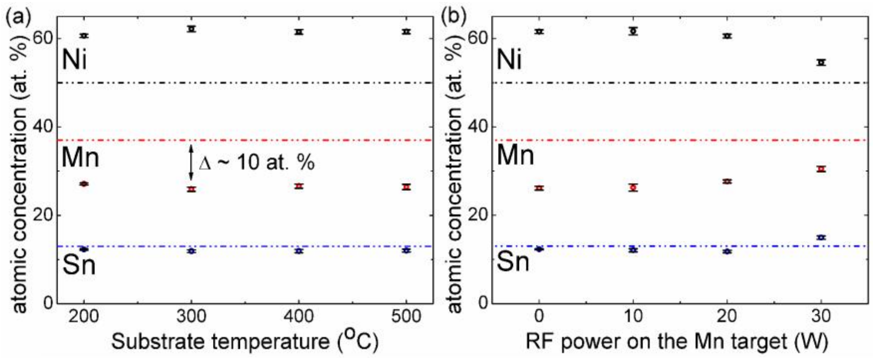

Fig. 1. Calculated average atomic concentration and standard deviation for Ni, Mn and Sn elements of the sputtered (a) and co-sputtered (b) films.thehorizontal dashed straight lines in the graphs represent the target elemental atomic composition Ni:Mn:Sn = 50:37:13

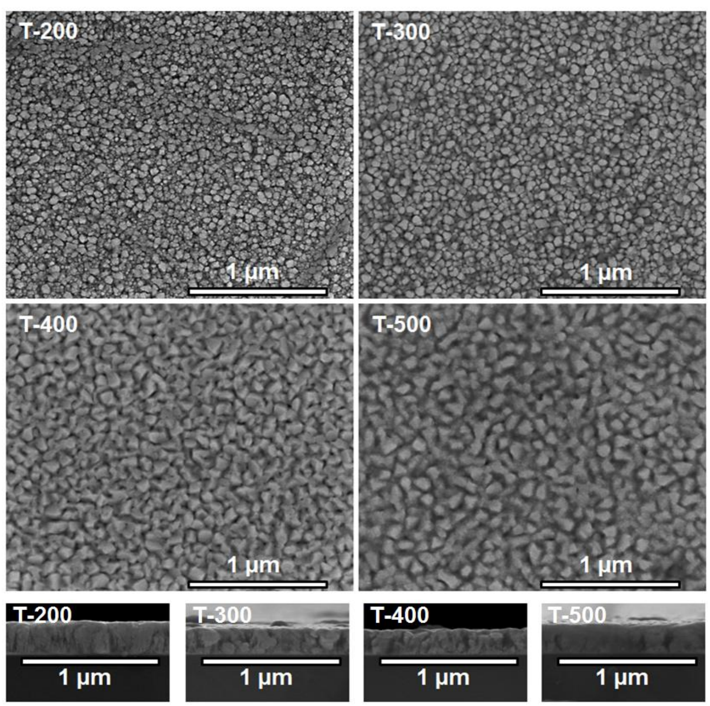

Fig. 2. SEM micrographs of the film surface and cross-sectional granular structure of T_200, T_300, T_400 and T_500 sputtered films

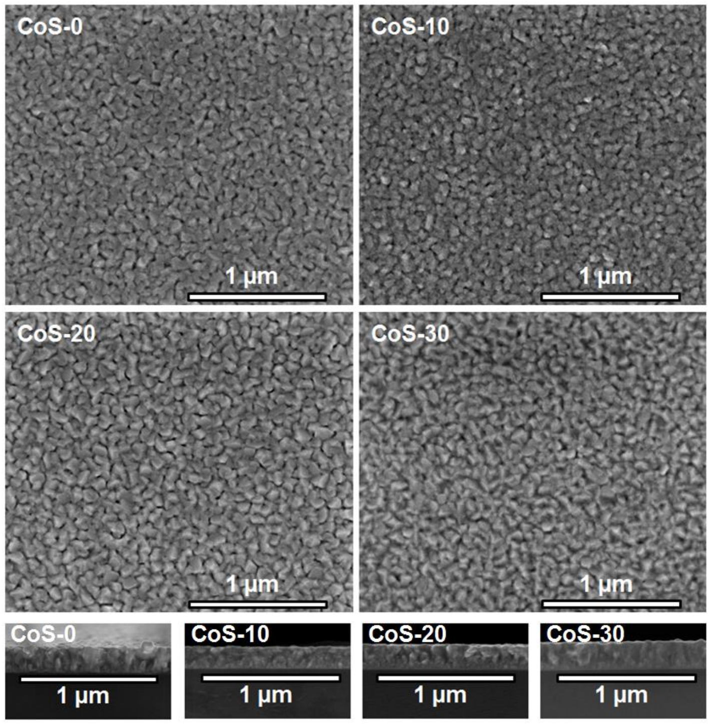

Fig. 3. SEM micrographs of the film surface and cross-sectional granular structure of CoS_0, CoS_10, CoS_20, and CoS_30 co-sputtered films

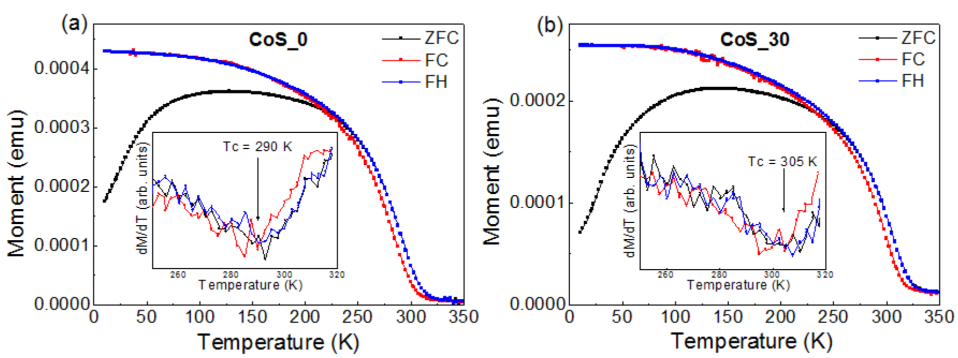

Fig. 4. ZFC, FC and FH *M(T)* curves measured under a constant applied magnetic field of 50 mT for CoS_0 and CoS_30 co-sputtered films. Inset: *dM/dT* vs. *T* curve

4. CONCLUSION

Studies in the *series T* thin films show a marked dependence of the average grain size on the substrate temperature, while the thickness and film composition remain almost unchanged in the range of the substrate temperatures here analyzed. In co-sputtered films microstructural features remain while the characteristic magnetic order temperature *Tc* shift from 290 K to 305 K when a 30 W of power is applied to the pure Mn RF cathode. This result is suggested to be as a consequence of the tailored film composition. From the preliminary study carried out it is concluded that the deposition of high quality thin films in the Ni-Mn-Sn Heusler alloys system with a desired granular structure and chemical composition requires both, a control of the substrate temperature and the co-sputtering deposition.

ACKNOWLEDGEMENTS

The authors acknowledge financial support received from: (a) CONACYT, Mexico, under projects CB-2010-01-157541 and CB-2012-176705; (b) ICyTDF, UACM, and Gobiernodel Distrito Federal-Mexico; (c) TUBITAK, Turkey (Research Fellowship Programme for Foreign Citizens). Technical support received from Laboratorio Nacional de Investigaciones en Nanociencias y Nanotecnología (LINAN, IPICYT), and M.Sc. G.J. Labrada-Delgado is also recognized. Carlos Garcia acknowledges the financial support by Fondecyt Grants No 1140552 and 1130950 and from project 111323 DGIP USM.

COMPETING INTERESTS

Authors have declared that no competing interests exist.

REFERENCES

1. Pecharsky VK, Gschneidner KA. Giant magnetocaloric effect in $Gd_5(Si_2Ge_2)$. Phys. Rev. Lett. 1997;78(23):4494-4497.
2. Pecharsky VK, Gschneidner KA, Tishin A. Thermodynamics of the magnetocaloric effect. Phys. Rev. B. 2001;64:144406.
3. Romero Gómez J, Ferreiro Garcia R, De Miguel Catoira A, Romero Gómez M. Magnetocaloric effect: A review of the thermodynamic cycles in magnetic refrigeration. Renew. Sustain. Energy Rev. 2013;17:74-82.
4. Recarte V, Pérez-Landazábal JI, Sánchez-Alárcos V, Chernenko VA, Ohtsuka M. Magnetocaloric effect linked to the martensitic transformation in sputter-deposited Ni–Mn–Ga thin films. Appl. Phys. Lett. 2009;95(14):141908.
5. Niemann R, Heczko O, Schultz L, Fähler S. Metamagnetic transitions and magnetocaloric effect in epitaxial Ni–Co–Mn–In films. Appl. Phys. Lett. 2010;97(22):222507.
6. Kariper İ.A., Production of HfO2 thin films using different methods: Chemical bath deposition, SILAR and sol–gel process, International Journal of Minerals, Metallurgy and Materials. 2014;21:832-838.
7. Auge A, Teichert N, Meinert M, Reiss G, Hütten A, Yüzüak E, Dincer I, Elerman Y, Ennen I, Schattschneider P. Thickness dependence of the martensitic transformation, magnetism, and magnetoresistance in epitaxial Ni-Mn-Sn ultrathin films. Phys. Rev. B. 2012;85(21):214118.
8. Vishnoi R, Kaur D. Size dependence of martensite transformation temperature in nanostructured Ni–Mn–Sn ferromagnetic shape memory alloy thin films. Surf. Coatings Technol. 2010;204(23):3773-3782.
9. Vishnoi R, Kaur D. Structural and magnetic properties of magnetron sputtered Ni–Mn–Sn ferromagnetic shape memory alloy thin films. J. Appl. Phys. 2010;107(10):103907.
10. Lee MD, Nong NV, Thuy NP, Yao YD, Lee SF, Liou Y, Chen YY, Wang C R. Temperature dependence of magnetic properties in Ni-Mn-Ga shape memory alloys. Phys. Status Solidi. 2004;1(12):3579-3582.
11. Annadurai A, Nandakumar AK, Jayakumar S, Kannan MD, Manivel Raja M, Bysak S, Gopalan R, Chandrasekaran V. Composition, structure and magnetic properties of sputter deposited Ni–Mn–Ga ferromagnetic shape memory thin films. J. Magn. Magn. Mater. 2009;321(6):630-634.
12. Chernenko VA, Kohl M, L'vov VA, Kniazkyi VM, Ohtsuka M, Kraft O. Martensitic Transformation and Microstructure of Sputter-Deposited Ni-Mn-Ga Films. Mater. Trans. 2006;47(3):619-624.
13. Zolotaryov A, Volland A, Heyn C, Novikov D, Stryganyuk G, Kornowski A, Vossmeyer T, Albrecht O, Coric E, Hansen W. Influence of growth temperature on phase and intermixing in Ni2MnIn Heusler films on InAs(001). J. Cryst. Growth. 2009;311(8):2397-2404.
14. Niemann R, Schultz L, Fähler S. Growth of sputter-deposited metamagnetic epitaxial Ni-Co-Mn-In films. J. Appl. Phys. 2012;111:093909.
15. Tillier J, Bourgault D, Odier P, Ortega L, Pairis S, Fruchart O, Caillault N, Carbone L. Tuning macro-twinned domain sizes and the b-variants content of the adaptive 14-modulated martensite in epitaxial Ni–Mn–Ga films by co-sputtering. Acta Mater. 2011;59(1):75-81.
16. Ekholm M, Larsson P, Alling B, Helmersson U, Abrikosov IA. Ab initio calculations and synthesis of the off-stoichiometric half-Heusler phase

$Ni_{1-x}Mn_{1+x}Sb$. J. Appl. Phys. 2010;108(9): 093712.
17. Valverde–Alva MA, García-Fernández T, Diáz-Cortés G, Sánchez-Llamazares JL, Rodríguez-González E, Sánchez-Aké C, Quintana-Nedelcos A, Villagrán-Muniz M.Expanded use of a fastphotographytechnique to characterize laser-induced plasma plumes. Rev. Mex. Fis. 2014;60:195-204.
18. Chung CY, Chernenko VA, Khovailo VV, Pons J, Cesari E, Takagi T. Thin films of ferromagnetic shape memory alloys processed by laser beam ablation. Mater. Sci. Eng. A. 2004;378(1-2):443-447.
19. Vishnoi R, Singhal R, Kaur D. Thickness dependent phase transformation of magnetron-sputtered Ni–Mn–Sn ferromagnetic shape memory alloy thin films. J. Nanoparticle Res. 2011;13(9): 3975-3990.
20. Tillier J, Bourgault D, Pairis S, Ortega L, Caillault N, Carbone L. Martensite structures and twinning in substrate-constrained epitaxial Ni–Mn–Ga films deposited by a magnetron co-sputtering process. Phys. Procedia. 2010;10:168-173.
21. Krenke T, Acet M, Wassermann E, Moya X, Mañosa L, Planes A. Martensitic transitions and the nature of ferromagnetism in the austenitic and martensitic states of Ni-Mn-Sn alloys. Phys. Rev. B. 2005;72(1):014412.
22. Zayak AT, Adeagbo WA, Entel P, Rabe, KM. *e⁄a* dependence of the lattice instability of cubic Heusler alloys from first principles. Appl. Phys. Lett. 2006;88: 111903.

Peer-review history:
The peer review history for this paper can be accessed here:
http://www.sciencedomain.org/review-history.php?iid=967&id=22&aid=8613